ELSEVIER

Catalysis Today 79–80 (2003) 211–218

CATALYSIS TODAY

www.elsevier.com/locate/cattod

Modeling of the Fischer–Tropsch synthesis in slurry bubble column reactors

Novica Rados[1], Muthanna H. Al-Dahhan*, Milorad P. Dudukovic

Chemical Reaction Engineering Laboratory, Washington University in St. Louis, Campus Box 1198, One Brookings Dr., St. Louis, MO 63130, USA

Abstract

A multicomponent one-dimensional dynamic mathematical model for the reacting slurry systems with a change in gas flow rate due to the chemical reaction is developed. A change in gas flow rate caused by the chemical reaction is modeled using the overall gas mass balance. Thus, all relevant chemical species are included in the model. Linear first-order reaction kinetics is considered. The gas phase is modeled using the two-bubble class hydrodynamic model. The interaction between small and large bubbles is included as the cross-flow. Suspension of liquid and solids is assumed to form a pseudo slurry phase. Back-mixing in all of the three considered phases, small bubbles, large bubbles and slurry, is accounted for using the axial dispersion model (ADM). Energy balance of the slurry phase is also included in the model. The developed general reacting slurry system model is used to simulate the performance of the Fischer–Tropsch (FT) slurry bubble column (SBC) reactor. Performance of the developed ADM based model is compared with the reactor scale models in which the reactor back-mixing is represented using some combination of the two limiting ideal reactor models of, complete stirred or plug flow.

Keywords: Multiphase reactors; Slurries; Dynamic simulation; Fischer–Tropsch; Gas conversion

1. Introduction

Slurry bubble column (SBC) reactors are presently used for a wide range of processes in both chemical and biochemical industry. These processes include [1]: oxidation, hydrogenation, chlorination, alkylation, polymerization [2], methanol and Fischer–Tropsch (FT) synthesis [3], etc. Sometime during this century the supply of crude oil may become short. Natural gas, especially from remote locations is presently unused and its price is relatively low. FT synthesis presents an interesting alternative for production of petro-chemicals and high quality diesel fuel (with high cetane number and virtually no sulfur). Advantages of the SBC reactors include: (1) nearly isothermal operation, (2) small solids particle size that results in good productivity, (3) good interface contacting, and (4) low pressure drop. Their superiority compared to other type of chemical reactors is specially pronounced in highly exothermic processes, like FT synthesis, when efficient interfacial contacting is needed and when the high level of back-mixing characteristic of SBC is beneficial to achieving good heat transfer and isothermality of operation. Hence, SBCs are among preferred reactor types for large scale FT processes.In SBC reactors, the phase back-mixing has been historically modeled using one of the two limiting ideal flow reactors, completely stirred tank (CST) or plug

* Corresponding author. Tel.: +1-314-935-7187; fax: +1-314-935-7211.
E-mail address: muthanna@wuche.wustl.edu (M.H. Al-Dahhan).
[1] Present address: ExxonMobil Research and Engineering, 3225 Gallows Road, Room 7A1938, Fairfax, VA 22037, USA.

0920-5861/03/$ – see front matter © 2003 Elsevier Science B.V. All rights reserved.
doi:10.1016/S0920-5861(03)00007-5

Nomenclature

a_W	cooling surface unit volume area (m^2_W/m^3_{SL})
A	arbitrary chemical specie
Be	reaction heat dimensionless group: $((-\Delta H_R)C_{G0}/\rho_{SL}C_{PSL}T_W He_A)$
c	dimensionless concentration (C/C_{G0})
C	concentration (mol/m^3)
C_P	heat capacity (J/kg K)
D	reactor diameter (m)
Da	Damkohler number ($k_R\varepsilon_L H_D/U_{G0}$)
E	axial dispersion coefficient (m^2/s)
f	ratio of the back-flow and the superficial flow in MCM models
g	gravity (9.80 m/s^2)
h_W	cooling surface convective heat transfer coefficient (J/m^2 K s)
H_D	reactor dynamic height (m)
He	Henry's solubility constant (m^3_{SL}/m^3_G)
ΔH_R	reaction heat (J/mol)
I	FT reactor inlet ratio ($c_{H_2,0}/c_{CO,0}$)
k	chemical reaction rate coefficient (s^{-1})
k_La	mass transfer coefficient (s^{-1})
K	bubble–bubble dimensionless interaction cross-flow coefficient
n	total number of chemical species considered in a modeled chemical process
N	number of continuously stirred tanks in the cascade (MCM model)
p_1, p_2, p_3	parameters defined in Eq. (4a–c)
p_{ST}	dimensionless static head pressure ($\rho_{SL}gH_D/P$)
P	pressure (Pa)
Pe_i	Peclet number ($U_{G0}H_D/E_i$)
Pe_H	heat Peclet number ($U_{G0}H_D\rho_{SL}C_{PSL}/\lambda_{SL}$)
R	ideal gas constant (8.314 J/mol K)
$St_{i,j}$	Stanton number ($(k_La)_i H_D/He_j U_{G0}$)
St_H	heat Stanton number ($h_W a_W H_D/\rho_{SL}C_{PSL}U_{G0}$)
t	time (s)
T	temperature (K)
u	dimensionless superficial velocity (U/U_{G0})
U	superficial velocity (m/s)
U_{FT}	FT reactor usage ratio ($\partial c_{H_2}/\partial c_{CO}$)
x	dimensionless axial position (z/H_D)
X_j	conversion of the specie j
z	axial position (m)

Greek letters

θ	dimensionless temperature (T/T_W)
ε	phase holdup ($m^3_{phase}/m^3_{reactor}$)
λ	heat conductivity (J/m K s)
ν_j	stoichiometric coefficient of the jth specie
ρ	density (kg/m^3)
σ	surface tension (kg/m s)
τ	dimensionless time (tU_{G0}/H_D)
Ω	parameter ($\Omega = 0.15544(U_G - U_{TR})^{-0.42}/D^{0.18}$)

Subscripts

0	inlet of the reactor
1	reference reactant
G	gas phase
j	chemical specie denominator
L	liquid phase
LB	large bubbles
SB	small bubbles
SL	slurry phase
T	total syn-gas
W	wall

flow (PF). More recently, the phase back-mixing is modeled using the axial dispersion model (ADM) [4,5] or the multi-cell model (MCM) [6]. Hartland and Mecklenburgh [7] analytically showed that the predictions of the ADM and MCM models are equivalent for $N \equiv (f + 1/2)Pe$. Schluter et al. [8] using a numerical simulation found the predictions of the ADM and MCM models to be similar. Degaleesan et al. [9] and Gupta et al. [10] introduced physically based convection–eddy diffusion two dimensional models for SBC and demonstrated their advantage in modeling dynamic tracer responses in SBC. Due to the popular use of the ADM, Degaleesan and Dudukovic [11] provided a method for proper evaluation of the axial dispersion coefficient for these models.

Dynamic models can be used for the simulation of the start-up, shut-down or transition operation (change

in the process set points). However, because of the computational complexity until recently SBC reactors have been exclusively modeled in the steady state operation. de Swart and Krishna [12] just recently proposed the first dynamic model of the FT SBC.

Fair amount of the actual chemical processes operate with a change in gas flow rate due to the chemical reaction (uneven number of reacted and produced moles) as in the FT process. Rigorous reactor scale model should calculate a change in gas flow rate by the overall mass or momentum balance accounting for all reacting gaseous species. In addition, because of the change in gas flow rate, changes in gas holdup have to be considered, too. This makes the rigorous model numerically involved and difficult to solve. Because of this reactor scale models with a change in the gas flow rate almost exclusively use a simplified approach based on linear dependency between the gas flow rate and conversion [13]. This approach is theoretically correct only in some limiting cases [14]. Thus, in most real industrial situations more realistic approach is needed.

Accordingly, the main objective of this work is to develop a one-dimensional dynamic model for the reacting SBC systems operated in the churn turbulent flow regime that properly accounts for a change in gas flow rate due to the chemical reaction. The change in gas flow rate is accounted for from the overall gas balance. As a case study, the performance of the Fischer–Tropsch SBC reactor is simulated using the developed model.

2. Reactor scale model

The developed one-dimensional dynamic model for the simulation of the performance of the SBC reactor has the following features. The flow is modeled as churn turbulent because many of the industrial slurry processes operate in this flow regime. In this operating regime the flow is represented with the three phases/cells (Fig. 1): small bubbles (SBs), large bubbles (LBs) and pseudo-slurry (SL) phase. Gas to liquid mass transfer is included as well as small and large bubbles interactions which are accounted for by the cross-flow mass exchange. Magnitude of these interactions is assumed to be finite and directly proportional to the slip velocity between the two (SB and

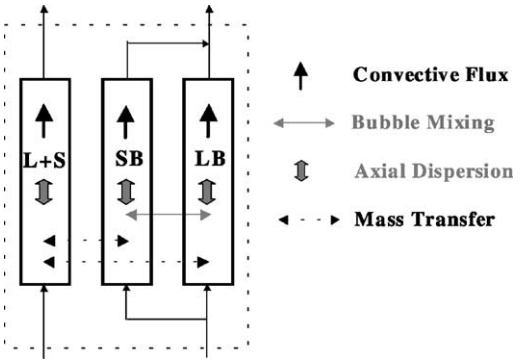

Fig. 1. Schematic representation of the slurry bubble column reactor scale model.

LB) bubble classes. Axial back-mixing (dispersion) is accounted for by the axial dispersion model (ADM).

Species mass balance equations are written in the dimensionless form. Species mass balance in small bubbles (solved for $c_{\mathrm{SB},j}$) written for $n-1$ species:

$$\varepsilon_{\mathrm{SB}}\frac{\partial c_{\mathrm{SB},j}}{\partial \tau} = -u_{\mathrm{SB}}\frac{\partial c_{\mathrm{SB},j}}{\partial x} - c_{\mathrm{SB},j}\frac{\partial u_{\mathrm{SB}}}{\partial x} - c_{\mathrm{SB},j}\frac{\partial \varepsilon_{\mathrm{SB}}}{\partial \tau} - (u_{\mathrm{LB}} - u_{\mathrm{SB}})K(c_{\mathrm{SB},j} - c_{\mathrm{LB},j}) - St_{\mathrm{SB},j}(c_{\mathrm{SB},j} - c_{\mathrm{L},j}) + \varepsilon_{\mathrm{SB}}Pe_{\mathrm{SB}}^{-1}\frac{\partial^2 c_{\mathrm{SB},j}}{\partial x^2} + Pe_{\mathrm{SB}}^{-1}\frac{\partial \varepsilon_{\mathrm{SB}}}{\partial x}\frac{\partial c_{\mathrm{SB},j}}{\partial x} \quad (1)$$

Species mass balance in large bubbles (solved for $c_{\mathrm{LB},j}$) written for $n-1$ species:

$$\varepsilon_{\mathrm{LB}}\frac{\partial c_{\mathrm{LB},j}}{\partial \tau} = -u_{\mathrm{LB}}\frac{\partial c_{\mathrm{LB},j}}{\partial x} - c_{\mathrm{LB},j}\frac{\partial u_{\mathrm{LB}}}{\partial x} - c_{\mathrm{LB},j}\frac{\partial \varepsilon_{\mathrm{LB}}}{\partial \tau} - (u_{\mathrm{LB}} - u_{\mathrm{SB}})K(c_{\mathrm{LB},j} - c_{\mathrm{SB},j}) - St_{\mathrm{LB},j}(c_{\mathrm{LB},j} - c_{\mathrm{L},j}) + \varepsilon_{\mathrm{LB}}Pe_{\mathrm{LB}}^{-1}\frac{\partial^2 c_{\mathrm{LB},j}}{\partial x^2} + Pe_{\mathrm{LB}}^{-1}\frac{\partial \varepsilon_{\mathrm{LB}}}{\partial x}\frac{\partial c_{\mathrm{LB},j}}{\partial x} \quad (2)$$

The concentration of the remaining specie in these cells/phases is calculated from the corresponding bubble (SB, LB) phase overall continuity balance equation:

$$c_{\mathrm{G}} = \sum_{j=1}^{n} c_{\mathrm{SB},j} = \sum_{j=1}^{n} c_{\mathrm{LB},j} = (1 + p_{\mathrm{ST}}(1-\varepsilon_{\mathrm{G}})(1-x))\frac{\theta_0}{\theta} \quad (3)$$

$$p_1 = -\frac{\varepsilon_G}{c_G} p_{ST}(1-x)\frac{\theta_0}{\theta} \quad (4a)$$

$$p_2 = \frac{u_G}{c_G} p_{ST}(1-\varepsilon_G)\frac{\theta_0}{\theta} \quad (4b)$$

$$p_3 = -(1-\varepsilon_{TR})\Omega U_{G0}\frac{u_G}{c_G} p_{ST}(1-x)\frac{\theta_0}{\theta} \quad (4c)$$

Species mass balance in liquid (solved for $c_{L,j}$) are written for all n species:

$$\varepsilon_{SL}\frac{\partial c_{L,j}}{\partial \tau} = -u_{SL}\frac{\partial c_{L,j}}{\partial x} - c_{SL,j}\frac{\partial \varepsilon_L}{\partial \tau} - St_{SB,j}He_j(c_{L,j} - c_{SB,j}) - St_{LB,j}He_j(c_{L,j} - c_{LB,j}) + \nu_j c_{L,1}\frac{DaSt_{S,1}}{St_{S,1} - \nu_1 Da}\frac{He_j}{He_1} + \varepsilon_{SL}Pe_{SL}^{-1}\frac{\partial^2 c_{L,j}}{\partial x^2} + Pe_{SL}^{-1}\frac{\partial \varepsilon_{SL}}{\partial x}\frac{\partial c_{L,j}}{\partial x} \quad (5)$$

In Eqs. (1)–(3) and (5), subscript j represents the jth specie of the chemical reaction $\sum_{j=1}^{n}\nu_j A_j = 0$ (for reactants: $\nu_j < 0$ and for products: $\nu_j > 0$). For modeling of the SBC FT reactor at the moment the only considered chemical reaction is the catalyst surface FT synthesis of the *n*-pentene pseudo product component:

$$H_2 + 0.5CO \overset{k_{FTS}}{\rightarrow} 0.1C_5H_{10} + 0.5H_2O \quad (6)$$

All other side reactions (including water gas shift reaction, WGS) are neglected at present. FT synthesis is taken to be first-order with respect to the reference reactant (H_2) concentration on the surface of solids. Dry [15] and Huff and Satterfield [16] showed that when hydrogen conversion is below 60% the first-order FT kinetics is a good approximation. Except in a few more detailed approaches [5] linear kinetics is used in most of the previous FT slurry models. Given the small solids particle size (50 μm and smaller) usually encountered in industrial slurry systems, intra-particle temperature and concentration profiles are most often negligible. Therefore, solids intra-particle mass and heat transfer resistances are presently neglected.

The change in gas flow rate (u_G) is calculated from the overall gas (includes both SB and LB) mass balance equation:

$$(1-\varepsilon_{TR})\Omega U_{G0}(1+p_1)\frac{\partial u_G}{\partial \tau} = -(1+p_3)\frac{\partial u_G}{\partial x} + \frac{\varepsilon_G}{\theta}\frac{\partial \theta}{\partial \tau} + \frac{u_G}{\theta}\frac{\partial \theta}{\partial x} + p_2 - \sum_{j=1}^{n}\frac{St_{SB,j}}{c_G}(c_{SB,j} - c_{SL,j}) - \sum_{j=1}^{n}\frac{St_{LB,j}}{c_G}(c_{LB,j} - c_{SL,j}) \quad (7)$$

In the present model, the total gas holdup, holdups and velocities of the two-bubble classes (SB and LB) are dependent on the SGV and the physical properties of the system. Therefore, they are treated as time and space (axial) dependent. Holdups and velocities as well as spatial and temporal derivatives of the two-bubble classes are calculated using the two-bubble class hydrodynamic model of Krishna and Ellenberger [17].

Two-bubble class models are relatively new approach in the reactor scale modeling of the churn turbulent bubble and SBCs [9,10]. They add more physics in the modeled representation of the gas flow. In last several years, two-bubble class models are almost exclusively used for the representation of the gas phase flow in the FT SBC reactors [5,18,23]. Assumption that all of the gas volume is present only in the form of small bubbles may lead (when the process is gas–liquid mass transfer controlled) to the overestimation of the conversion because of the much larger unit volume area that is in this case available for the gas–liquid mass transfer. However, if one accounts for the two-bubble classes but does not account for the finite SB–LB interactions the calculated conversion may be smaller than the actual. The large amount of the gas that is present in large bubbles in this case practically bypasses the reactor since the unit volume area available for the LB–L mass transfer is much lower than the area for the SB–L mass transfer.

Change in temperature (θ) is calculated using the slurry phase energy balance:

$$\varepsilon_{SL}\frac{\partial \theta}{\partial \tau} = -u_{SL}\frac{\partial \theta}{\partial x} - St_H(\theta - 1) - \nu_1 c_{SL,1}Be\frac{DaSt_{S,1}}{St_{S,1} - \nu_1 Da} + \varepsilon_{SL}Pe_H^{-1}\frac{\partial^2 \theta}{\partial x^2} + Pe_H^{-1}\frac{\partial \varepsilon_{SL}}{\partial x}\frac{\partial \theta}{\partial x} \quad (8)$$

All liquid–solid interfacial heat transfer resistances are neglected. Slurry phase is assumed to be in thermal equilibrium with the gas phases. Because of vigorous mixing in the churn turbulent SBCs these assumptions are justified.The initial conditions for model equations are consistent with the boundary conditions. The initial specie concentrations in the three considered phases (SB, LB, L) are set to the inlet concentrations of the species in the gas phase. Gas at the reactor inlet contains only reactants. Initially, and at the reactor inlet, liquid is saturated with the gas phase. The inlet boundary conditions for the specie concentrations and temperature are of the Danckwerts type. At the outlet boundary conditions are zero mass and thermal fluxes [19]. Needed physical properties are taken from the work of Mills et al. [19]. Henry constants are given by Peter and Weinert [20] and diffusivities of all species (needed for calculation of the L–S mass transfer, St_S) are calculated using the correlation of Wilke and Chang [21]. The cross-flow parameter, K, for the lack of better estimate is kept at 5. This value of K results in moderate SB–LB interactions.

3. FT process simulation results

Figs. 2–4 show the transient profiles at the reactor outlet and the steady state operation axial profiles for two different inlet ratios ($I = 0.5$ for hydrogen lean and $I = 2.0$ for stoichiometric syn-gas composition) and at two different reactor diameters ($D = 0.05$ and 0.50 m). Given the stoichiometry of the studied FT kinetics (Eq. (6)) in the steady state operation the usage ratio (U_{FT}, ratio of the reacting quantities of hydrogen and carbon monoxide) of the process is 2.

In Fig. 2, inlet ratio of only 0.5 is studied. In other words the process is lacking hydrogen and is therefore hydrogen controlled. Because of that extent of

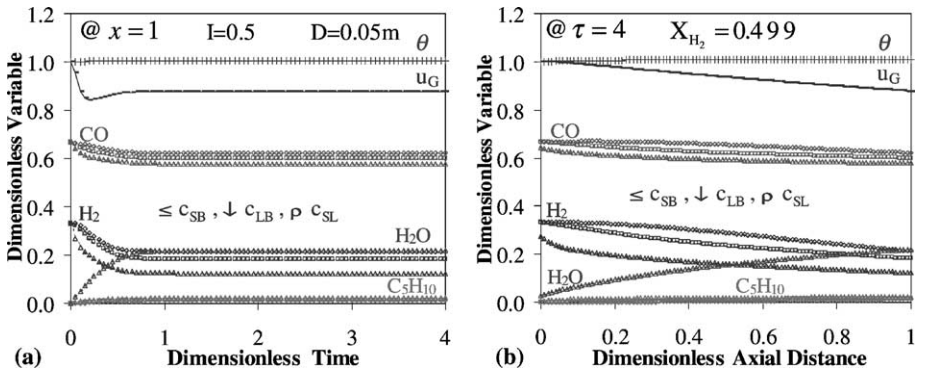

Fig. 2. FT time (a) and axial (b) profiles ($X_{H_2} = 0.499$). $I = 0.5$, $U_G = 0.10$ m/s, $U_{SL} = 0.02$ m/s, $H_D = 5$ m, $D = 0.05$ m.

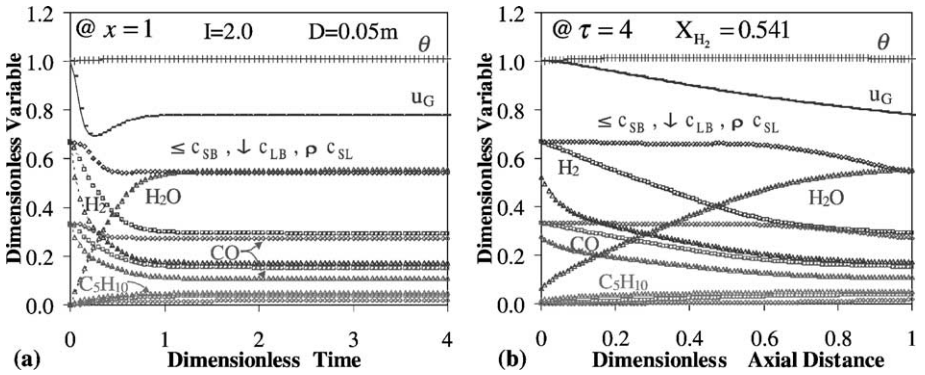

Fig. 3. FT time (a) and axial (b) profiles ($X_{H_2} = 0.541$). $I = 2.0$, $U_G = 0.10$ m/s, $U_{SL} = 0.02$ m/s, $H_D = 5$ m, $D = 0.05$ m.

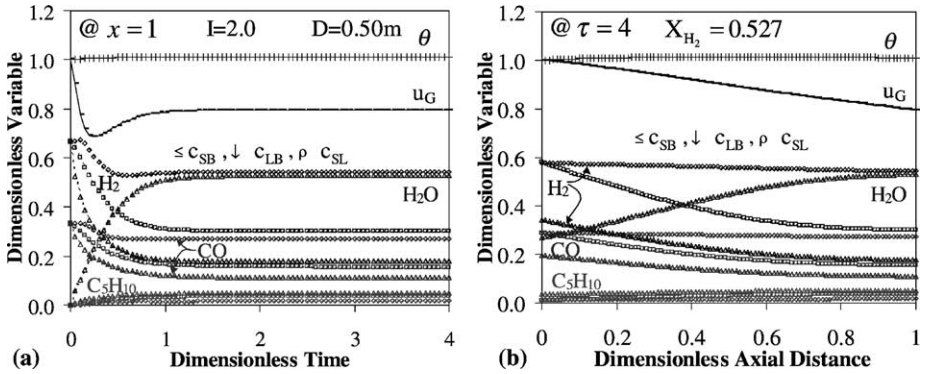

Fig. 4. FT time (a) and axial (b) profiles ($X_{H_2} = 0.527$). $I = 2.0$, $U_G = 0.10$ m/s, $U_{SL} = 0.02$ m/s, $H_D = 5$ m, $D = 0.05$ m.

the reaction is low (concentration gradients in Fig. 2 are low). Although half of the available hydrogen is consumed ($X_{H_2} = 0.499$):

$$X_{H_2} = 1 - \frac{u_{SB}c_{SB,H_2} + u_{LB}c_{LB,H_2} + u_L c_{L,H_2} He_{H_2}^{-1}}{1 + u_L He_{H_2,0}^{-1}} \times \frac{I+1}{I} \quad (9a)$$

$$X_T = \frac{1+I}{1+U_{FT}} X_{H_2} \quad (9b)$$

The total syn-gas conversion (X_T) is only 0.250.

When the inlet ratio is increased to 2 (stoichiometric ratio) although the hydrogen conversion increases only slightly to 0.541 the total syn-gas conversion jumps to the same value of 0.541 (Fig. 3) resulting in steeper concentration profiles. In both of these two cases, reactor diameter is taken to be 0.05 m, representative of bench scale column simulating the case of negligible axial back-mixing (flow is close to the PF).

Fig. 4 considers the wider reactor of 0.50 m. This larger diameter in contrast to previous two cases exhibits considerable back-mixing. The flow is now well-mixed causing the concentration profiles to be more flat. Still, despite considerable back-mixing conversion fell marginally to 0.527. From industrial point of view, this is good since large diameter rectors needed for the large volume production can be used comparably well with just small loss in performance (also see Fig. 5). Practically, uniform time and axial temperature profiles obtained in all three studied cases (Figs. 2–4) suggest that the total cooling area is large enough to absorb the generated FT reaction heat (which is considerable at 200 kJ/mol). This result agrees with previous studies [19,22] and confirms the well known fact that due to the good mixing properties SBC FT reactors offer relatively easy heat removal with less cooling area than some other types of FT reactors (e.g. trickle bed).

In order to maximize the conversion taller reactors with larger residence times are needed (Fig. 5). Gas velocity should be as small as optimally possible in order to increase the reactant residence time but high enough to keep the flow in the churn turbulent regime insuring good mass and heat transfer (Fig. 6). Small superficial slurry velocity needed for continuous liquid product removal can be used since it does not decrease the performance considerably compared to the batch

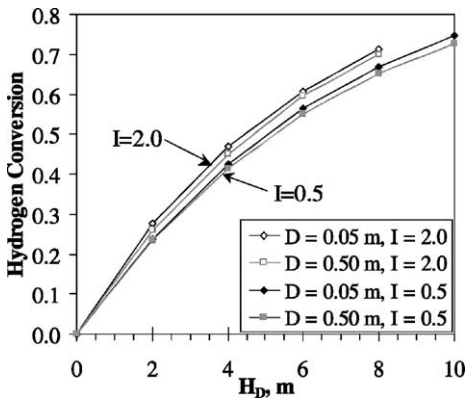

Fig. 5. The effect of reactor height and diameter on hydrogen conversion in FT synthesis. $U_G = 0.10$ m/s, $U_{SL} = 0.02$ m/s.

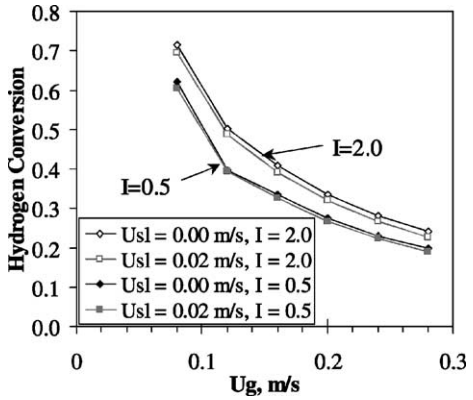

Fig. 6. The effect of gas and liquid superficial velocity on hydrogen conversion in FT synthesis. $H_D = 5\,m$, $D = 0.05\,m$.

slurry operation (Fig. 6). When the extent of WGS reaction is negligible (as when using catalysts with low WGS activity) the inlet ratio should be as close to the mean usage ratio as possible to maximize the conversion.

4. The effect of back-mixing on the FT SBC reactor performance

Predicted performance obtained using developed FT SBC full axial dispersion model (SB, LB and L are modeled using ADM) is compared to the predicted performance of several models composed of a combination of ideal reactor modes (PF and CST). PF and CST models are simulated using the present model by setting the value of Pe^{-1} to 0 and 10^4, respectively. It is found that in a narrow reactor of 0.05 m in diameter full PF model (SB, LB, SL in PF mode) matches the performance (hydrogen conversion) of the developed full ADM model within 1%. This is expected as the narrow diameter reactors exhibit negligible back-mixing. Indeed, the other ideal reactor models performed much worse (differences above 9%). In the moderate 0.50 m reactor diameter full PF and G-PF, SL-CST models approach the full ADM model within 5%. The extent of back-mixing is largest in the 2.0 m diameter reactor of low aspect ratio. However, even in this reactor the observed specie concentration profiles are still not completely invariant along the height as in the CST reactor. The full ADM model conversion is matched the best using G-PF, SL-CST or LB-PF, SB-CST, SL-CST models (within 5%). Obviously, the conversion of the full ADM model can be fairly well matched with some ideal reactor model for any of the considered three reactor diameters, 0.05, 0.50 and 2.00 m. However, the closest combination of ideal reactor models varies with the reactor diameter and the extent of actual back-mixing. Thus, in order to use the correct ideal reactor model one would need to, a priori, based on the column diameter and other parameters, estimate the extent of back-mixing. Full CST model that is often used in industry is about 7% off in matching the full ADM model hydrogen conversion even in the almost completely back-mixed 2.00 m diameter reactor.

For all considered reactor diameters the spread in predicted conversions between the PF and CST models is about 20%. Hence, this is the maximum deviation (for this set of operating and inlet conditions resulting in relatively modest conversion) in predicted conversion when the back-mixing modes for different phases are not well selected. Unfortunately, just matching the conversion is not a proof that the two models with different combination of back-mixing modes predict the same concentration profiles, too.

The outcome of this comparison does not mean that the full ADM model is better than some ideal reactor model. It simply shows that the full ADM model is more versatile than the ideal rector modeling approach. However, the success of the ADM model in accurate simulation of the experimental data depends on the accuracy of the correlations that are used for calculation of Peclet numbers in different phases. If these correlations are not accurate or are non-existent the advantage of ADM model disappears. In this case, ideal reactor model consisting of G-PF and SL-CST or G-PF and SL-PF for very slender reactors should be used.

5. Summary

A dynamic SBC reactor scale model has been developed. The change in gas flow rate caused by the chemical reaction is calculated from the total gas mass balance. Therefore, all relevant gaseous chemical species are considered in the model. The full advantages of this model can only be realized when more accurate and detailed kinetic scheme is used.

Conversion in FT SBC reactor is effected the most by the mean residence time. Increase in reactor diameter increases phase back-mixing, but its effect on conversion is relatively small and is greatly compensated by the benefits of the large throughput operation. Small slurry superficial velocity that is necessary for the continuous wax product removal decreases the conversion negligibly compared to the batch operation. Inlet syn-gas composition should be close to the expected mean usage ratio since its effect on conversion is considerable.

Present full ADM model is shown to be more versatile than the ideal reactor models. If the Peclet number correlations are inaccurate or non-existent the best results are obtained when modeling the gas phase in a PF mode and slurry phase in a CST mode (or a PF mode for narrow reactors). Ideal reactor model in which all phases are in CST mode should not be used. Its predictions are found to be off compared to the present model even for the very large 2.0 m diameter reactor.

References

[1] W.-D. Deckwer, E. Alper, Katalytische Suspensions Reacktoren, Chem. Eng. Technol. 52 (1980) 219.
[2] Y.T. Shah, B.G. Kelkar, S.P. Godbole, W.-D. Deckwer, Design parameter estimation for bubble column reactors, AIChE J. 28 (1982) 353.
[3] M.E. Dry, The SASOL route to fuels, ChemTech 12 (1982) 744.
[4] J.R. Turner, P.L. Mills, Comparison of axial dispersion and mixing cell models for design and simulation of Fischer–Tropsch slurry Bubble column reactors, Chem. Eng. Sci. 45 (1990) 2317.
[5] G.P. van der Laan, A.A.C.M. Beenackers, R. Krishna, Multicomponent reaction engineering model for Fe-catalyzed Fischer–Tropsch synthesis in commercial scale slurry bubble column reactors, Chem. Eng. Sci. 54 (1999) 5013.
[6] T.M. Leib, P.L. Mills, J.J. Lerou, J.R. Turner, Evaluation of neural networks for simulation of three-phase bubble column reactors, Chem. Eng. Res. Des. 73 (A6) (1995) 690.
[7] S. Hartland, J.C. Mecklenburgh, A comparison of differential and stagewise counter current extraction with back-mixing, Chem. Eng. Sci. 21 (1966) 1209.
[8] S. Schluter, A. Steiff, P.-M. Weinspach, Modeling and simulation of bubble column reactors, Chem. Eng. Process. 31 (1992) 97.
[9] S. Degaleesan, M.P. Dudukovic, B.A. Toseland, B.L. Bhatt, A two-compartment convective diffusion model for slurry bubble column reactors, Ind. Eng. Chem. Res. 36 (11) (1997) 4670.
[10] P. Gupta, B. Ong, M.H. Al-Dahhan, M.P. Dudukovic, B. Toseland, Hydrodynamics of churn turbulent bubble columns: gas–liquid recirculation and mechanistic modeling, Catal. Today 64 (3–4) (2001) 253.
[11] S. Degaleesan, M.P. Dudukovic, Liquid back-mixing in bubble columns and the axial dispersion coefficient, AIChE J. 44 (11) (1998) 2369.
[12] J.W.A. de Swart, R. Krishna, Simulation of the transient and steady state behavior of a bubble column slurry reactor for Fischer–Tropsch synthesis, Chem. Eng. Process. 41 (2002) 35.
[13] Levenspiel, O., 1972. Chemical Reaction Engineering, second ed. Wiley, New York.
[14] D. Stern, A.T. Bell, H. Heinemann, A theoretical model for the performance of bubble-column reactors used for Fischer–Tropsch synthesis, Chem. Eng. Sci. 40 (1985) 1665.
[15] M.E. Dry, Advances in Fischer–Tropsch chemistry, Ind. Eng. Chem. Prod. Res. Dev. 15 (1976) 282.
[16] G.A. Huff Jr., C.N. Satterfield, Intrinsic kinetics of the Fischer–Tropsch synthesis on a reduced fused-magnetite catalyst, Ind. Eng. Chem. Process Des. Dev. 23 (1984) 696.
[17] R. Krishna, J. Ellenberger, Gas holdup in bubble column reactors operating in the churn turbulent flow regime, AIChE J. 42 (1996) 2627.
[18] C. Maretto, R. Krishna, Modeling of a bubble column slurry reactor for Fischer–Tropsch synthesis, Catal. Today 52 (1999) 279.
[19] Mills, P.L., Turner, J.R., Ramachandran, P.A., Dudukovic, M.P., 1996. The Fischer–Tropsch Synthesis in Slurry Bubble Column Reactors: Analysis of Reactor Performance Using the Axial Dispersion Model. Topics in Chemical Engineering, vol. 8. Gordon and Breach, London.
[20] S. Peter, M. Weinert, Uberdie Loslichkeit von H_2, CO, CO_2, und Wasserdampf in Flussigen Kohlenwasserstoffen, Z. Phys. Chem. 5 (1955) 114.
[21] C.R. Wilke, P. Chang, Correlation of diffusion coefficients in dilute solutions, AIChE J. 1 (1955) 164.
[22] W.-D. Deckwer, Y. Serpemen, M. Ralek, B. Schmidt, Modeling of the Fischer–Tropsch synthesis in the slurry phase, Ind. Eng. Chem. Process Des. Dev. 21 (1982) 231.
[23] de Swart, J.W.A., 1996. Scale-up of a Fischer–Tropsch slurry reactor. Ph.D. Thesis, University of Amsterdam, The Netherlands.